Changes in Iron Use during the 2nd and 1st Millennia B.C. at Kaman-Kalehöyük, Turkey: Composition of Iron Artifacts from Stratum III and Stratum II

Hideo AKANUMA
Iwate

1 INTRODUCTION

Since 1986, twenty annual seasons of archaeological excavation have been conducted at the site of Kaman-Kalehöyük in central Anatolia, Turkey, by the Japanese Institute of Anatolian Archaeology. Four main cultural strata have been identified[1] and a large number of archaeological objects and structures have been discovered, establishing the cultural chronology of the site.

Archaeometallurgical analyses of iron objects from Kaman-Kalehöyük have been carried out by the author over ten years in order to develop an understanding of the changes in iron use and manufacture during the 2nd and 1st millennia B.C. In 2002, three small fragments of iron artifacts, two of them with the composition of steel, were discovered in Stratum IIIc, dating to the Assyrian Colony Period (Akanuma 2002). These objects are some six hundred years older than the period of Stratum IIIa, the Hittite Empire Period. This indicates that iron use may have begun in the Assyrian Colony Period. It is necessary to clarify the acquisition details of those three iron objects.

Fragments of iron artifacts with the composition of steel were also found in Stratum IIIb (the Old Hittite Kingdom Period) and Stratum IIIa (the Hittite Empire Period) (Akanuma 2005). In Stratum IIIa, small lumps of slag, roughly the size of a thumb, were also excavated (Akanuma 1995a; 1995b). This means that some kind of iron production process was most likely performed at the site at the time of the Hittite Empire Period. A progressive increase in the deposits of iron artifacts, lumps, and slag has been recorded in the Stratum II (Iron Age) levels (Akanuma 1999); in particular, large iron tools were discovered in Stratum IIa (Omura 1998). This indicates that iron processing and manufacturing advanced in the cultural age of Stratum II, especially Stratum IIa.

Based on the results of archaeometallurgical analysis, it is believed that the means of procuring smelted iron, smelted and refined iron, or iron objects as final products may have changed along with political and economic fluctuations in the central Anatolian region during the periods corresponding to Stratum III and Stratum II at Kaman-Kalehöyük. However, the acquisition method of those iron materials and objects, and the actual conditions of use of iron at the site in the 2nd and 1st millennia B.C. are not clear. In order to resolve this problem, it is helpful to classify iron artifacts from the site based on archaeometallurgical analysis and compare them to iron objects excavated from other sites. In this paper, I will examine the results of archaeometallurgical analysis of iron objects excavated from Stratum IIIb, IIc and IIa levels at Kaman-Kalehöyük in 2004, also taking into consideration previous archaeometallurgical studies.

---

[1] At Kaman-Kalehöyük, four main cultural levels have been identified: Stratum I, Ottoman Period (16th to 17th centuries A.D.); Stratum II, the Iron Age (end of the second millennium to the second half of the first millennium B.C.); Stratum III, Middle to Late Bronze Ages (the second millennium B.C.); and Stratum IV, Early Bronze Age (the third millennium B.C.) (Omura 1995). Stratum I, Stratum II, and Stratum III are divided into two, four, and three substrata respectively, from youngest to oldest, Stratum Ia and Ib, Stratum IIa, IIb, IIc, and IId, Stratum IIIa (the Hittite Empire Period), IIIb (the Old Hittite Kingdom Period), and IIIc (the Assyrian Colony Period) (Omura 1995; 2003).

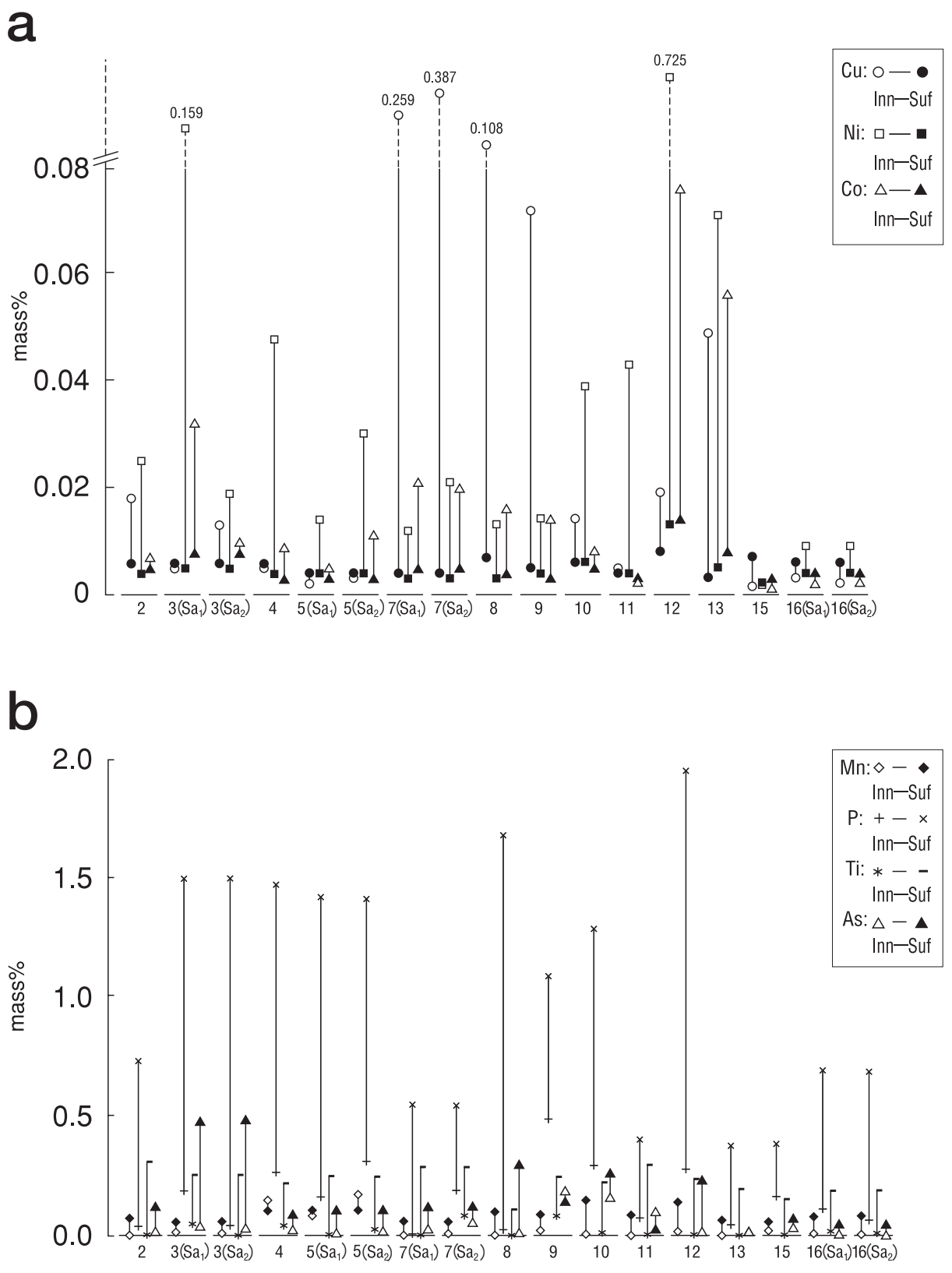

Fig.1 Comparison of the chemical composition between the inner sample（Inn） and the surface sample (Suf) extracted from the same iron artifact. a:Comparison of the Cu, Ni, and Co contents.b: Comparison of the Mn, P, Ti, and As contents.

Table 1 Examined iron objects

No.	Object	Description of Excavation					Stratum
		Sector	Grid	Date	Provisional Layer	Structure	
1	Iron ore	North VIII	XXXI-55	040705	⑥①	P2697	IIIb
2	Fragment	North XIX	XXXVI-57	040805	㉒	-	IIa
3	Fragment			040805		-	
4	Fragment	North XVI	XXXIV-52	040813	⑤⑤	-	
5	Fragment of knife		XXXV-52	040827	④⑧	H250	
6	Iron slag	North X	XXVII-55	040825	⑳	-	
7	Pin-like object		XXVI-54	040903		-	
8	Fragment	North XVIII	XXXIX-56	040907	④②	P2270	
9	Nail						
10	Fragment						
11	Fragment						
12	Fragment						
13	Fragment	North XXXII	XLIII-50	040909	⑰	P2802	
14	Fragment	South LVI	LII-49	040903	⑲	P755	IIc
15	Pin			040906			
16	Objects		LIII-48	040908	㉗	-	
17	Fragment		LIII-49	040920		-	

2 ARCHAEOLOGICAL OBJECTS

Seventeen iron objects excavated from Kaman-Kalehöyük in 2004 were examined. Table 1 lists the archaeological provenience data for each object.[2)] Sample No.1 was found in a Stratum IIIb pit (P 2697). Samples No.2 to No.13 were found in Stratum IIa and Samples No.14 to No.17 in Stratum IIc.

Samples No.2 to No.5 and No.7 to No.17 are iron artifacts. It was difficult to discern exactly what they were, as they were covered with soil or were highly corroded. Before extracting samples from them, x-ray transmission photography was carried out. The soil and iron corrosion products were removed using a portable drill equipped with a diamond cutting wheel. The external appearances of these fifteen samples (after conservation treatment) are shown in Figs.2 to 6. Sample No.5 (Fig.4$b_{1\text{-}1}$) is part of a knife, No.9 (Fig.5b_1) a nail, and No.15 a pin (Fig.6$d_{1\text{-}1}$). It is difficult to identify the original forms of the other twelve samples. Sample No.1 (Fig.7a_1) is a lump found to be composed mainly of hematite. Sample No.6 (Fig.8a_1) is a blackish-brown lump of iron slag that also contains iron corrosion products.

3 SAMPLE PREPARATION

Samples of approximately 100-200mg were taken from the iron artifacts, approximately 1000mg from slag and ore. This was performed using a portable drill equipped with a diamond cutting wheel. V-shaped cuts were put in the ore and slag, and then the samples for analysis were extracted from them. Each extracted sample was divided into two parts: the larger part was used for metallographic observation, and the smaller part was used for chemical analysis.

The surfaces of thirteen of the iron artifacts were covered with a great deal of soil (Samples No.2 to No.5, No.7 to No.13, No.15, and No.16). Therefore, samples for chemical analysis were extracted from the surface in addition to the inner portion, to consider the influence of contamination from the burial deposits. Surface samples, indicated by “Suf,” are composed mainly of soil and a

2) The description of excavation and estimated dates Stratum listed in Table 1 are according to research by Dr. Sachihiro Omura and his co-workers.

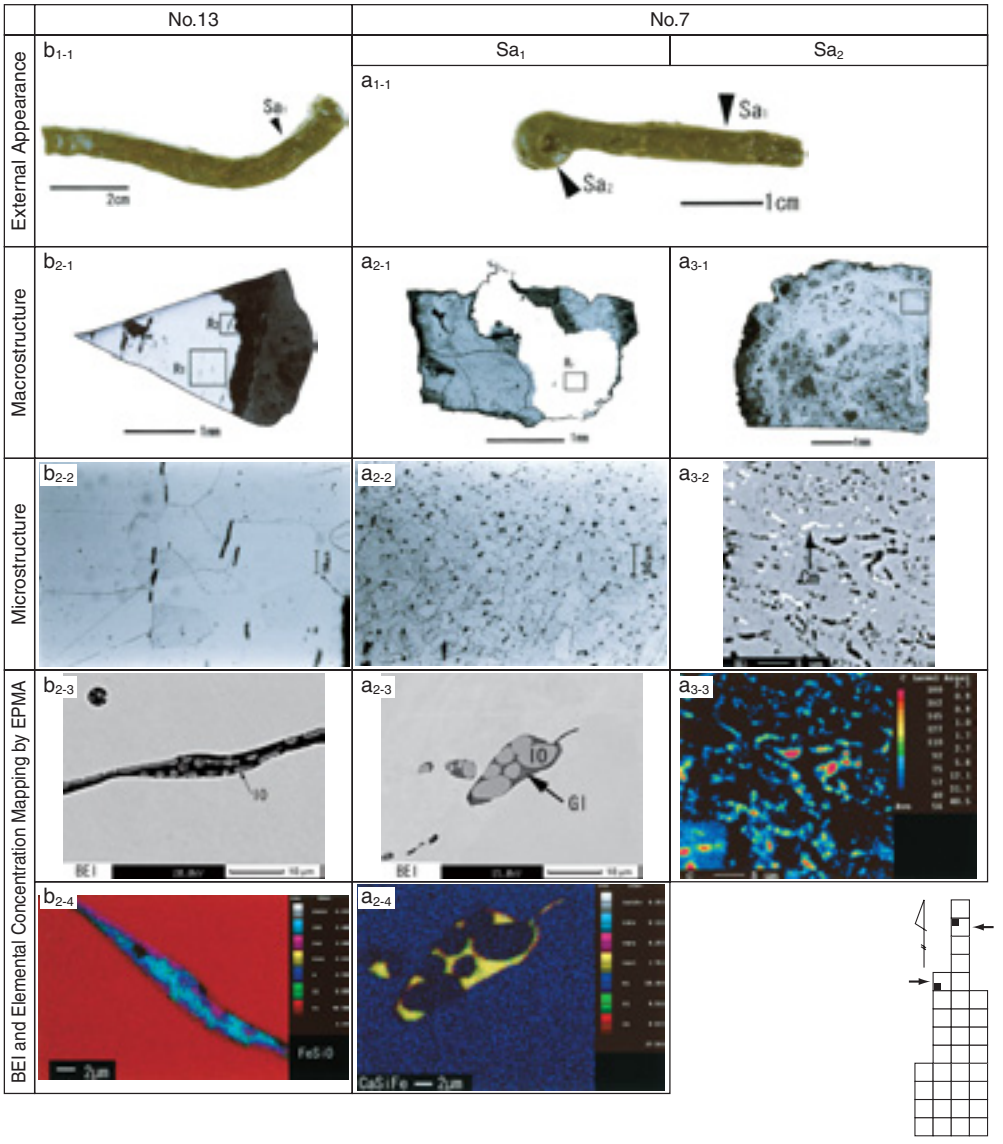

Fig.2 External appearance and metallographic analysis of Samples No.7 and No.13 excavated from Stratum IIa.a_{1-1}: External appearance of Sample No.7.b_{1-1}: External appearance of Sample No.13. The metallographic samples were extracted from the marked locations in each external appearance.a_{2-1} and b_{2-1}: Macrostructures etched with nital.a_{2-2} and b_{2-2}: Microstructures of the areas 'R_1' in a_{2-1} and b_{2-1}.a_{3-1}: Macrostructure of No.7Sa_2.a_{3-2} and a_{3-3}: EPMA backscattered electron image (BEI) and elemental concentration mapping of the area 'R_1' in a_{3-1}. Cm: cementite or its holes.a_{2-3}, a_{2-4}, b_{2-3}, and b_{2-4}: EPMA backscattered electron images and elemental concentration mapping of the area 'R_1' in a_{2-1} and the area 'R_2' in b_{2-1}, respectively. IO: iron oxide (estimated to be wüstite), Gl: glassy silicates. (Excavation plan from Omura 2005)

small amount of corrosion products; inner samples are indicated by "Sa_1." Two inner samples (Sa_1 and Sa_2) were extracted from different areas of Samples No.3, No.5, No.7, and No.16 to examine variation in chemical composition. The external corrosion layers of Samples No.14 and No.17 were removed with a diamond-coated wheel to avoid contamination from burial deposits.

4 ANALYTICAL METHODS USED

The samples to be used for metallographic observation were sectioned, mounted with epoxy resin, ground with emery paper and then polished using diamond paste. The prepared samples were then examined under an optical microscope. Electron

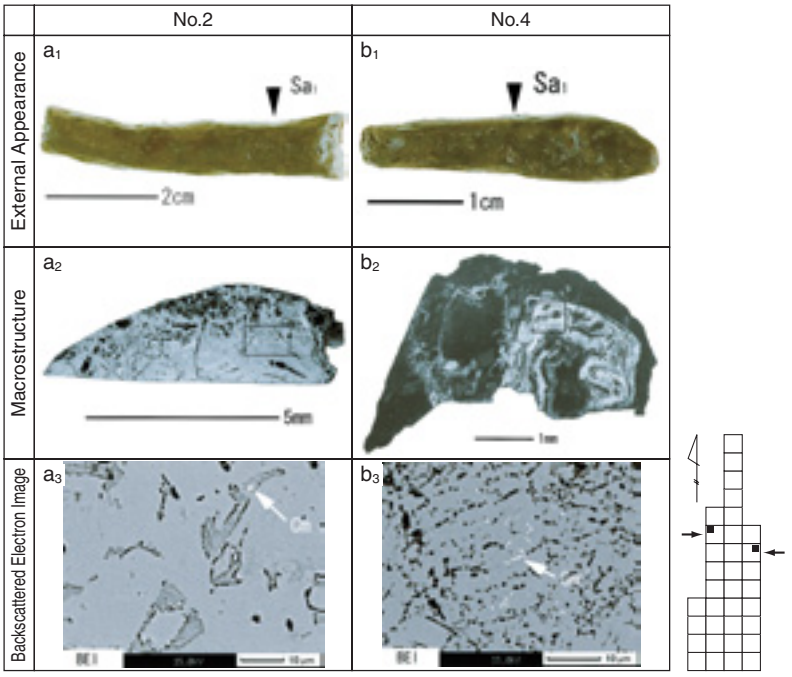

Fig.3 External appearance and metallographic analysis of Samples No.2 and No.4 excavated from Stratum IIa. The metallographic samples were extracted from the marked locations in each external appearance.a_2 and b_2: Macrostructures.a_3 and b_3: EPMA backscattered electron images of the marked locations in each macrostructure. Cm: cementite or its holes. (Excavation plan from Omura 2005)

microprobe analyses (EPMA) were performed with a JEOL JXA-8100, equipped with three wavelength-dispersing x-ray spectrometers, in order to examine the microstructure and to identify the mineral phase compositions of non-metallic inclusions. Since Samples No.7Sa_2 and No.13 had large areas of metallic iron, they were etched with nital (2.5ml HNO_3 and 97.5ml EtOH) before optical examination, after EPMA analysis.

Inductively coupled plasma optical emission spectroscopy (ICP-OES) using a PERKIN ELMER Optima 4300DV was employed for the chemical analysis of fifteen elements in the samples. The elements determined, and the analytical lines selected (nm), were as follows: Fe (239.562), Cu (324.752), Ni (231.604), Co (228.616), Mn (257,610), P (213,617), Ti (334.940), Si (251.611), Ca (317.929), Al (396.153), Mg (285.213), V (290.880), As (193.696), Sb (206.836), and Mo (202.031). Sulfur in Sample No.13 was tested by an infrared absorption

Table 2 Composition of iron artifacts and lumps by ICP-OES, IRA, and EPMA

No.	Sub. No.	chemical components(mass%)																elements ratios				m.s.	n.m.i.
		T.Fe	Cu	Ni	Co	Mn	P	Ti	Si	Ca	Al	Mg	V	As	Sb	Mo	S	Co*(Co/Ni)	Cu*(Cu/Ni)	Ni**(Ni/Co)	Cu**(Cu/Co)		
2	Sa_1	58.84	0.018	0.025	0.007	0.001	0.04	0.004	0.60	2.38	0.062	0.224	0.002	0.02	<0.01	0.010	-	0.28	0.72	3.57	2.57	Cm(0.3-0.4)	no
	Suf	9.67	0.006	0.004	0.005	0.073	0.73	0.310	19.5	5.27	5.02	0.917	0.035	0.12	<0.01	0.002	-	-	-	-	-	-	-
3	Sa_1	59.40	0.005	0.159	0.032	0.011	0.19	0.050	1.71	0.324	0.443	0.106	0.003	0.04	<0.01	0.006	-	0.20	0.03	4.97	0.16	Cm	no
	Sa_2	41.50	0.013	0.019	0.010	0.006	0.04	0.002	0.27	0.196	0.025	0.038	<0.001	0.02	<0.01	0.003	-	0.53	0.68	1.90	1.30	no	Gl
	Suf	14.97	0.006	0.005	0.008	0.056	1.50	0.253	18.1	3.09	4.38	0.671	0.080	0.49	<0.01	0.005	-	-	-	-	-	-	-
4	Sa_1	83.51	0.005	0.048	0.009	0.149	0.26	0.041	5.31	2.00	1.59	0.274	0.007	0.03	<0.01	0.004	-	0.19	0.10	5.33	0.56	Cm(0.1-0.2)	no
	Suf	6.35	0.006	0.004	0.003	0.104	1.47	0.217	17.6	8.56	4.34	0.810	0.032	0.09	<0.01	0.001	-	-	-	-	-	-	-
5	Sa_1	64.72	0.002	0.014	0.005	0.083	0.16	0.004	0.50	0.221	0.070	0.074	0.003	0.01	<0.01	0.003	-	0.36	0.14	2.80	0.40	no	Gl
	Sa_2	56.76	0.003	0.030	0.011	0.166	0.31	0.025	1.94	2.68	0.572	0.349	0.010	0.02	<0.01	0.007	-	0.37	0.10	2.73	0.27	no	no
	Suf	9.13	0.004	0.004	0.003	0.108	1.42	0.247	17.1	6.56	4.59	0.806	0.050	0.11	<0.01	0.002	-	-	-	-	-	-	-
7	Sa_1	97.54	0.259	0.012	0.021	<0.001	<0.01	0.004	0.12	0.042	0.019	0.006	<0.001	0.03	<0.01	0.001	-	1.75	21.6	0.57	12.3	Pa(0.1-0.2)	Gl,(IO,Gl)
	Sa_2	54.20	0.387	0.021	0.020	0.008	0.19	0.089	3.39	0.389	1.02	0.150	0.008	0.05	<0.01	0.001	-	0.95	18.4	1.05	19.4	Cm(0.1-0.2)	no
	Suf	15.92	0.005	0.003	0.005	0.059	0.55	0.287	18.0	3.34	4.76	0.682	0.033	0.13	<0.01	0.001	-	-	-	-	-	-	-
8	Sa_1	74.24	0.108	0.013	0.016	0.004	0.03	0.002	0.31	0.117	0.013	0.037	<0.001	0.01	<0.01	0.004	-	1.23	8.31	0.81	6.75	no	no,Cu-p
	Suf	10.01	0.007	0.003	0.004	0.097	1.68	0.108	20.4	4.07	5.48	0.523	0.035	0.30	<0.01	0.001	-	-	-	-	-	-	-
9	Sa_1	63.40	0.072	0.014	0.014	0.019	0.49	0.082	4.07	3.14	0.908	0.448	0.021	0.19	<0.01	0.008	-	1.00	5.14	1.00	5.14	no	Gl
	Suf	6.90	0.005	0.004	0.003	0.087	1.09	0.245	17.8	4.97	4.32	0.806	0.026	0.15	<0.01	0.001	-	-	-	-	-	-	-
10	Sa_1	66.38	0.014	0.039	0.008	0.007	0.29	0.011	0.98	0.540	0.239	0.112	0.003	0.16	<0.01	0.026	-	0.21	0.36	4.88	1.75	Cm	no
	Suf	8.71	0.006	0.006	0.005	0.149	1.29	0.221	16.7	6.33	4.22	0.907	0.045	0.26	<0.01	0.002	-	-	-	-	-	-	-
11	Sa_1	69.54	0.005	0.043	0.002	0.001	0.07	0.008	0.55	0.263	0.138	0.063	0.001	0.10	<0.01	0.009	-	0.05	0.12	-	-	Cm(0.3-0.4)	Gl
	Suf	3.28	0.004	0.004	0.003	0.082	0.40	0.296	20.1	6.18	5.40	0.866	0.012	0.03	<0.01	<0.001	-	-	-	-	-	-	-
12	Sa_1	62.54	0.019	0.725	0.076	0.017	0.28	0.006	0.17	2.02	0.131	0.213	0.002	0.02	<0.01	0.002	-	0.10	0.03	9.54	0.25	no	no
	Suf	8.34	0.008	0.013	0.014	0.139	1.95	0.234	18.0	6.64	4.12	0.861	0.044	0.23	<0.01	<0.001	-	-	-	-	-	-	-
13	Sa_1	98.67	0.049	0.071	0.056	<0.001	0.04	0.002	0.05	0.014	0.009	0.003	<0.001	0.01	<0.01	0.003	0.076	0.79	0.69	1.27	0.88	Pa(<0.1)	IO,Gl
	Suf	3.51	0.003	0.005	0.008	0.064	0.38	0.193	15.0	11.4	4.10	0.954	0.006	0.01	<0.01	<0.001	-	-	-	-	-	-	-
14	Sa_1	70.39	0.002	0.004	0.001	0.009	0.10	0.002	0.55	0.265	0.051	0.096	0.006	0.02	<0.01	0.001	-	-	-	-	-	no	no
15	Sa_1	58.64	0.001	0.002	0.001	0.021	0.16	0.004	0.51	0.317	0.064	0.153	0.011	0.04	<0.01	0.002	-	-	-	-	-	no	no
	Suf	32.02	0.007	0.002	0.003	0.058	0.39	0.151	11.3	2.52	2.54	0.499	0.051	0.07	<0.01	0.001	-	-	-	-	-	-	-
16	Sa_1	60.77	0.003	0.009	0.002	0.007	0.11	0.019	1.88	1.80	0.473	0.208	<0.001	0.01	<0.01	0.002	-	0.22	0.33	-	-	Cm(0.2-0.3)	IO,Gl
	Sa_2	60.54	0.002	0.009	0.002	0.008	0.06	0.011	0.66	1.87	0.131	0.276	<0.001	<0.01	<0.01	0.001	-	0.22	0.22	-	-	Cm(0.2-0.3)	no
	Suf	12.08	0.006	0.004	0.004	0.080	0.69	0.187	16.8	6.38	3.91	0.745	0.022	0.05	<0.01	0.001	-	-	-	-	-	-	-
17	Sa_1	84.46	0.187	0.002	0.017	0.007	0.04	0.013	0.92	0.214	0.293	0.068	<0.001	0.01	<0.01	0.005	-	-	-	0.12	11.0	no	Gl,Cu-P

The numbers refer to sample descriptions in Table 1. Pa and Cm represent pearlite and cementite, respectively.
The parenthesized numerals are the estimated carbon contents from the microstructure. m.s. and n.m.i represent microstructure and non-metallic inclusion, respectively.
IO:Fe-O system compound, Gl:glassy silicate, Ma: a glassy silicate with minute crystals in it,and Cu-p:copper particles.

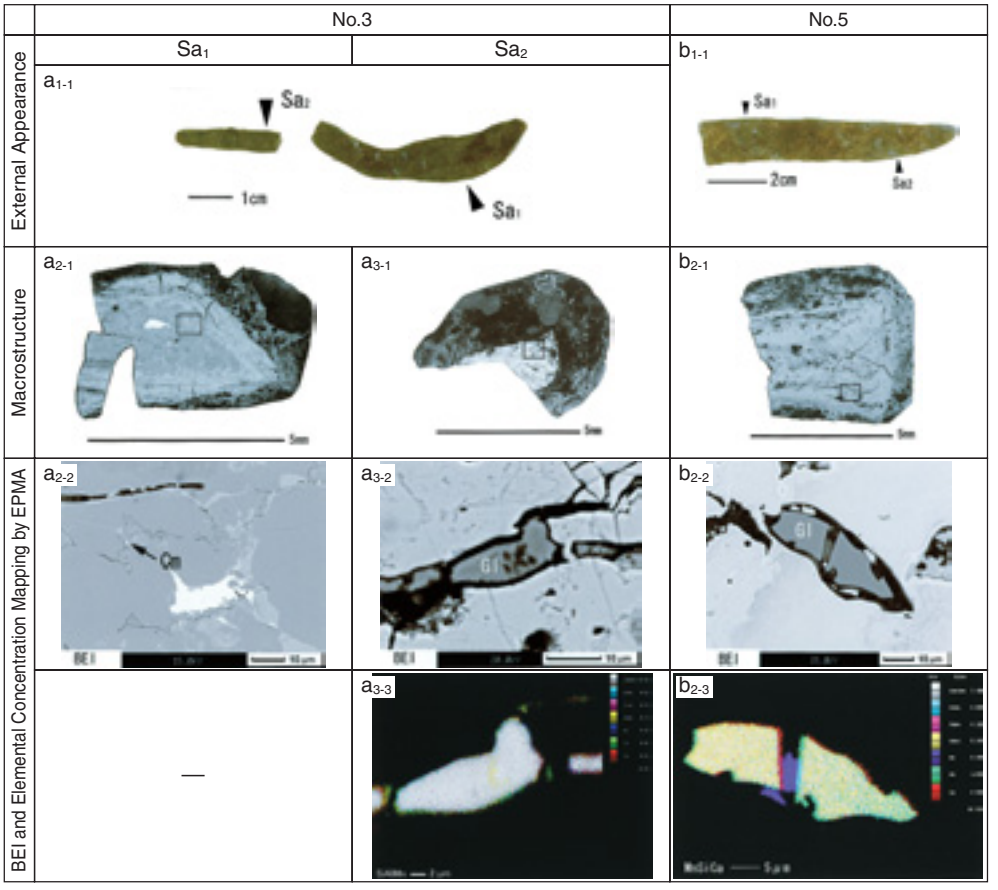

Fig.4 External appearance and metallographic analysis of Samples No.3 and No.5 excavated from Stratum IIa.a_{1-1} and b_{1-1}: External appearance of Samples No.3 and No.5.The metallographic samples were extracted from the marked locations in each external appearance. a_{2-1}, a_{3-1}, and b_{2-1}: Macrostructures of each sample.a_{2-2}, a_{3-2}, and b_{2-2}: EPMA backscattered electron images of the marked areas of a_{2-1}, a_{3-1}, and b_{2-1}, respectively. Cm: cementite or its holes. Gl: glassy silicates.a_{3-3} and b_{2-3}: EPMA elemental concentration mapping of a_{3-2} and b_{2-2}. (Excavation plan from Omura 2005)

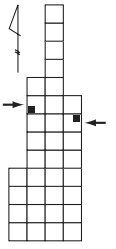

method (IRA) after combustion in a current of oxygen, using a LECO CS444. FeO content in Samples No.1 and No.5 was analyzed by titrimetric analysis. The analytical procedures and operating conditions were the same as in Akanuma (2001).

5 ANALYTICAL RESULTS

5-1 Chemical composition of iron artifacts

Table 2 reports the analytical data obtained by ICP-OES and IRA. The total iron (T.Fe) content in Samples No.7Sa_1 and No.13Sa_1 are 97.54mass% and 98.67mass%, respectively, indicating that the samples consist mainly of metallic iron. Samples No.4Sa_1 and No.17Sa_1 are believed to contain both metallic iron and iron corrosion, because the T.Fe content is between 83mass% and 85mass%.The other fifteen samples from the inner portions of iron artifacts are composed mainly of iron corrosion, as indicated by their T.Fe content of less than 75mass%.

In well-preserved Samples No.7Sa_1 and No.13Sa_1, the element composition is believed to reflect the original composition of the object. However, in the case of the corroded samples, there may be contamination of trace elements from the surrounding soil. The contents

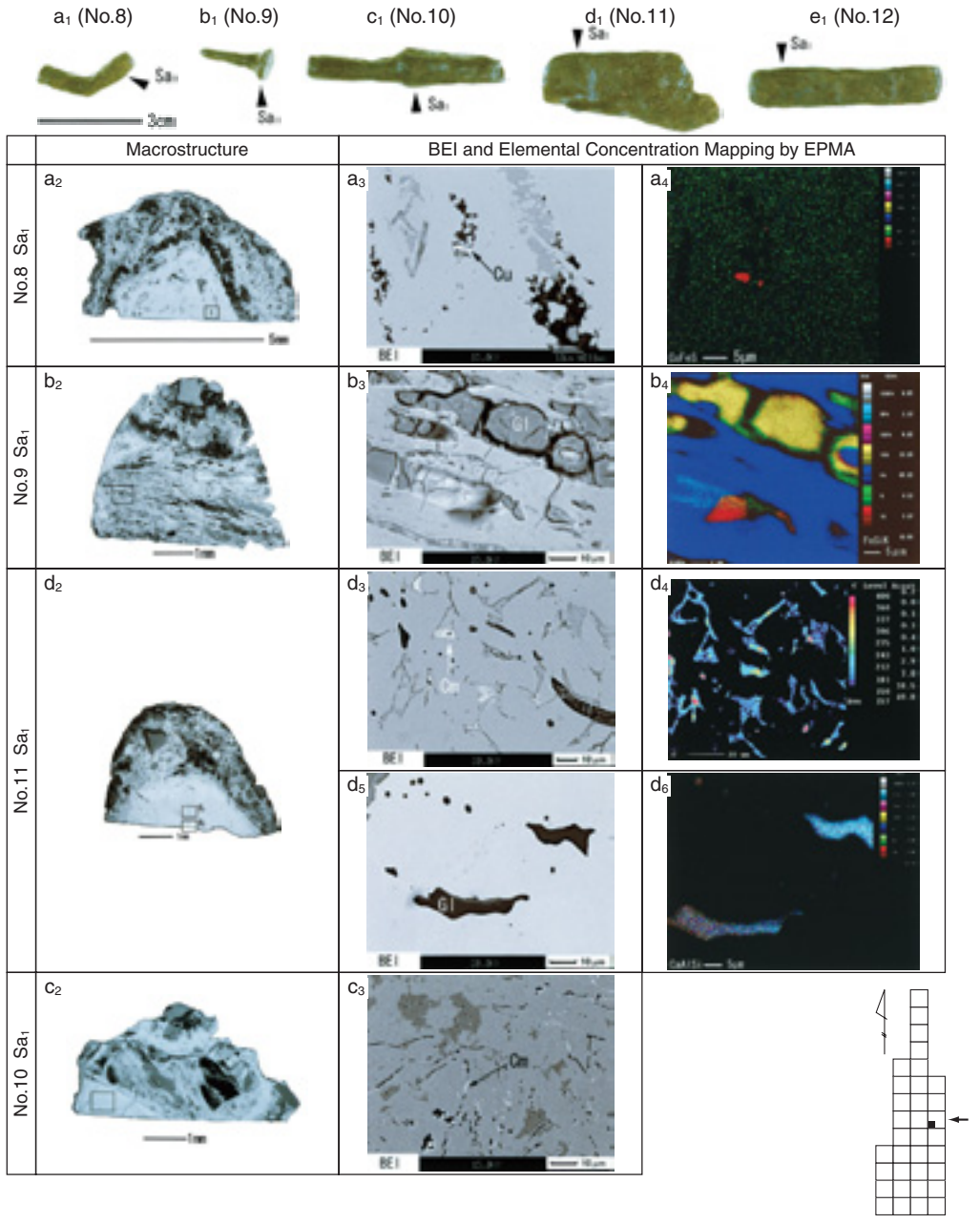

Fig.5 External appearance and metallographic analysis of Samples No.8 to No.12 excavated from Stratum IIa.a_1 to e_1: External appearances of Samples No.8 to No.12. The metallographic samples were extracted from the marked locations in each external appearance.a_2 to d_2: Macrostructures of each sample.a_3 to d_3 and d_5: EPMA backscattered electron images of the marked areas in a_2 to d_2, respectively. Cm: cementite or its holes, Gl: a glassy silicate. a_4, b_4, d_4, and d_6: EPMA elemental concentration mapping of a_3, b_3, c_3, and d_5, respectively. (Excavation plan from Omura 2005)

of Cu, Ni, Co, Mn, P, Ti, and As were examined to determine the extent of contamination from the soil.

Fig.1a shows the Cu, Ni, and Co concentrations detected in the seventeen inner samples and thirteen surface samples extracted from each object. Fig.1b shows the Mn, P, Ti, and As concentrations of the same. The values of Cu, Ni, and Co in many inner samples are higher than those in the surface portion of each sample. However, in many other inner samples, the values of Cu, Ni, and Co are equal to or lower than what they are in the corresponding surface portion of each sample. See Table 2.

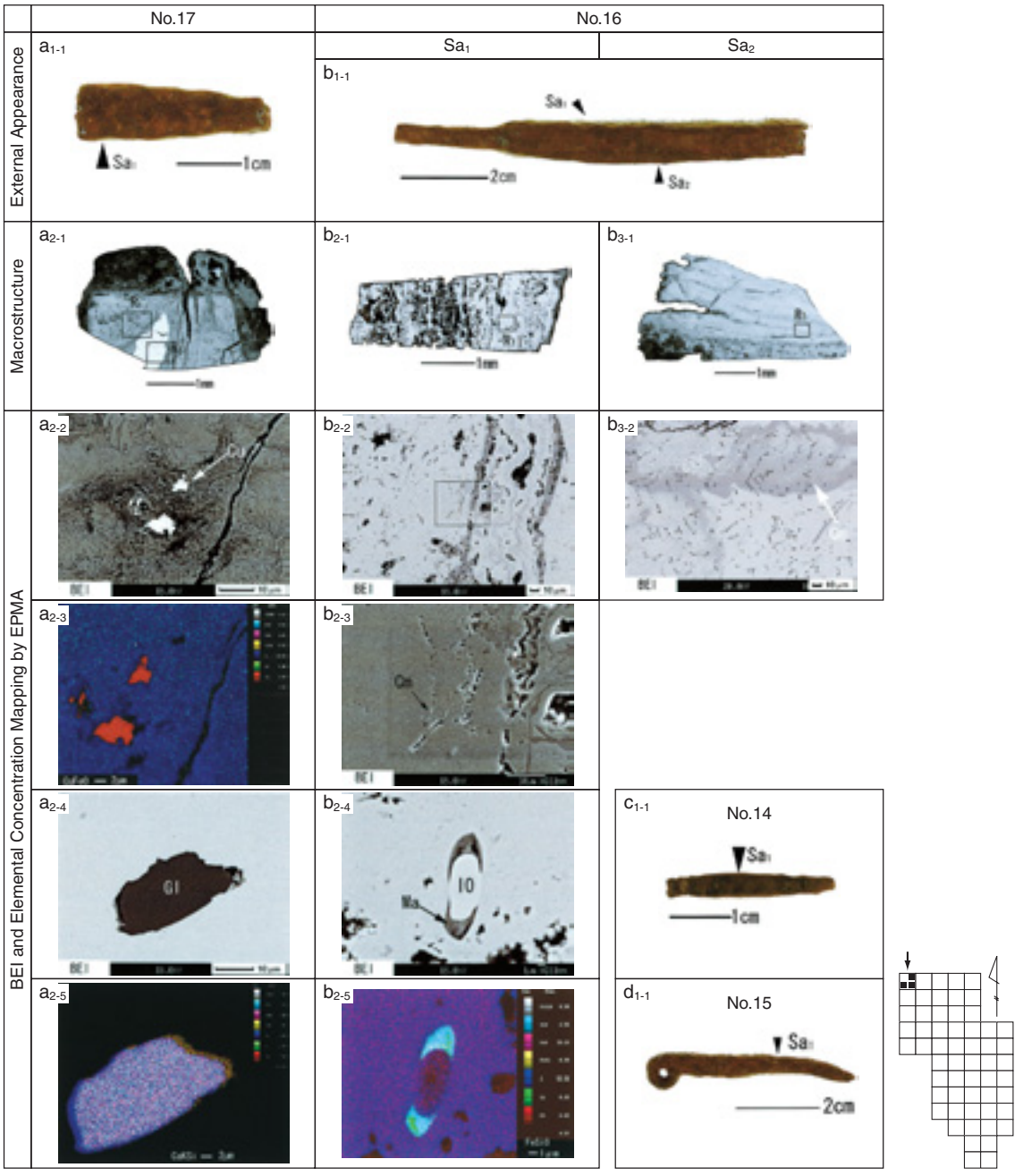

Fig.6 External appearance and metallographic analysis of Samples No.14 to No.17 excavated from Stratum IIc.a_{1-1}, b_{1-1}, c_{1-1}, and d_{1-1}: External appearances of Samples No.17, No.16, No.14, and No.15, respectively. The metallographic samples were extracted from the marked locations in each external appearance.a_{2-1}, b_{2-1}, and b_{3-1}: Macrostructures of each sample.a_{2-2}, b_{2-2} and b_{3-2}: EPMA backscattered electron images of the areas 'R_1' in a_{2-1}, b_{2-1} and b_{3-1}, respectively.b_{2-3}: Backscattered electron image of the marked area of b_{2-2} by EPMA. Cm: Cementite or its holes.a_{2-3}: EPMA elemental concentration mapping of a_{2-2}.a_{2-4} and b_{2-4}: EPMA backscattered electron images of the areas 'R_2' in a_{2-1} and b_{2-1}, respectively. IO: iron oxide (believed to be wüstite), Gl:a glassy silicate. Ma: a glassy silicate containing minute particles.a_{2-5} and b_{2-5}: EPMA elemental concentration mapping of the non-metallic inclusions in a_{2-4} and b_{2-4}, respectively. (Excavation plan from Omura 2005)

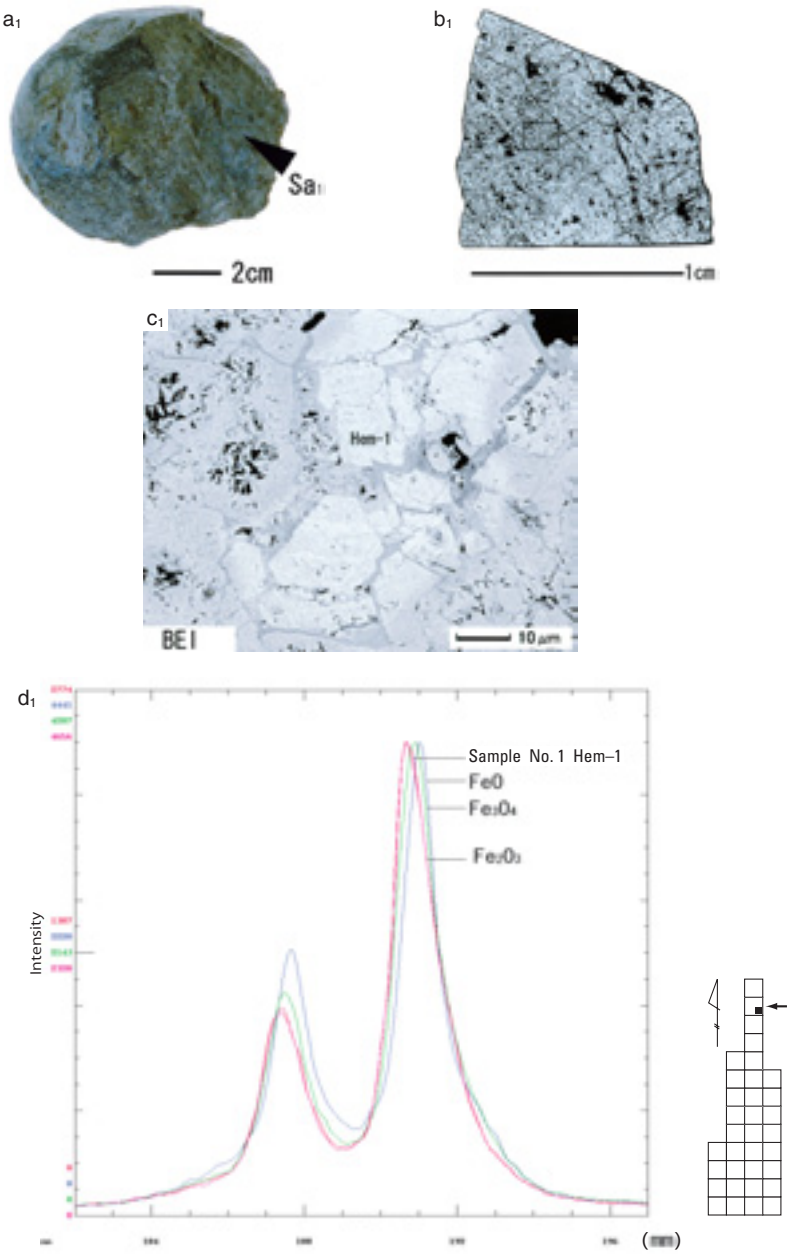

Fig.7 External appearance and metallographic analysis of Sample No.1 excavated from Stratum IIIb.a_1: External appearance. The metallographic samples were extracted from the marked location.b_1: Macrostructure.c_1: Backscattered electron image of the marked area in b_1 by EPMA.d_1: Spectra of Fe-L α and Fe-L β of Hem-1 in c_1 and standard samples of iron oxide.

Samples No.14 and No.15 are considered to have been in approximately the same burial environment, since they were found in the same excavation grid and the same layer. Sample No.15Sa_1 is more corroded than Sample No.14Sa_1, based on its lower T.Fe content, so might be expected to be more affected by soil contaminants. However, the contents of Cu, Ni, and Co in Sample No.15Sa_1 are equal to or lower than those of Sample No.14Sa_1, indicating that Sample No.15Sa_1 does not appear to have been contaminated by Cu, Ni, or Co from the surrounding soil. For Samples No.16 and No.17, the same explanation applies. Therefore, we believe the concentrations of Cu, Ni, and Co in most of the samples originate from the objects themselves,

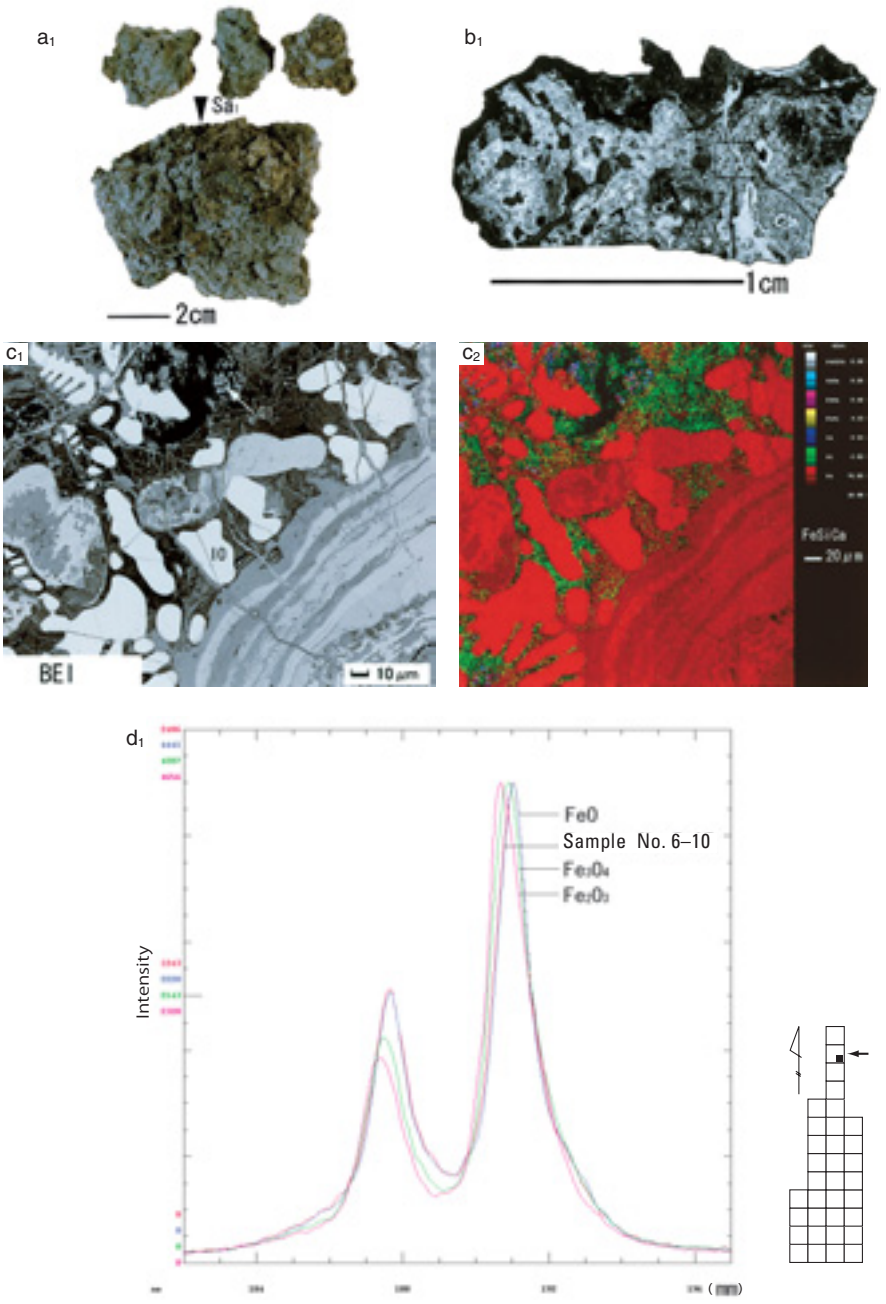

Fig.8 External appearance and metallographic analysis of Sample No.6 excavated from Stratum IIa.a_1: External appearance of Sample No.6.b_1: Macrostructure.c_1 and c_2: Backscattered electron image and elemental concentration mapping of the marked area in b_1 by EPMA. IO: iron oxide (believed to be wüstite), Gl: glassy silicates.d_1: Spectra of Fe-L α and Fe-L β of IO in c_1 and standard samples of iron oxide.

specifically from the raw iron materials used to make them. In some samples, it is difficult to judge the influence of burial contaminants, but when the trace element content in the inner samples is less than 0.005mass%, that influence is believed to be poor.

As shown in Fig.1b, the contents of P and Ti in all thirteen surface samples, and the contents of Mn and As in eleven surface samples, are equal to or higher than those of each corresponding inner sample. This indicates that Ti, Mn, P, and As are not useful in classifying iron materials, as they may be contaminants from the surrounding soil.

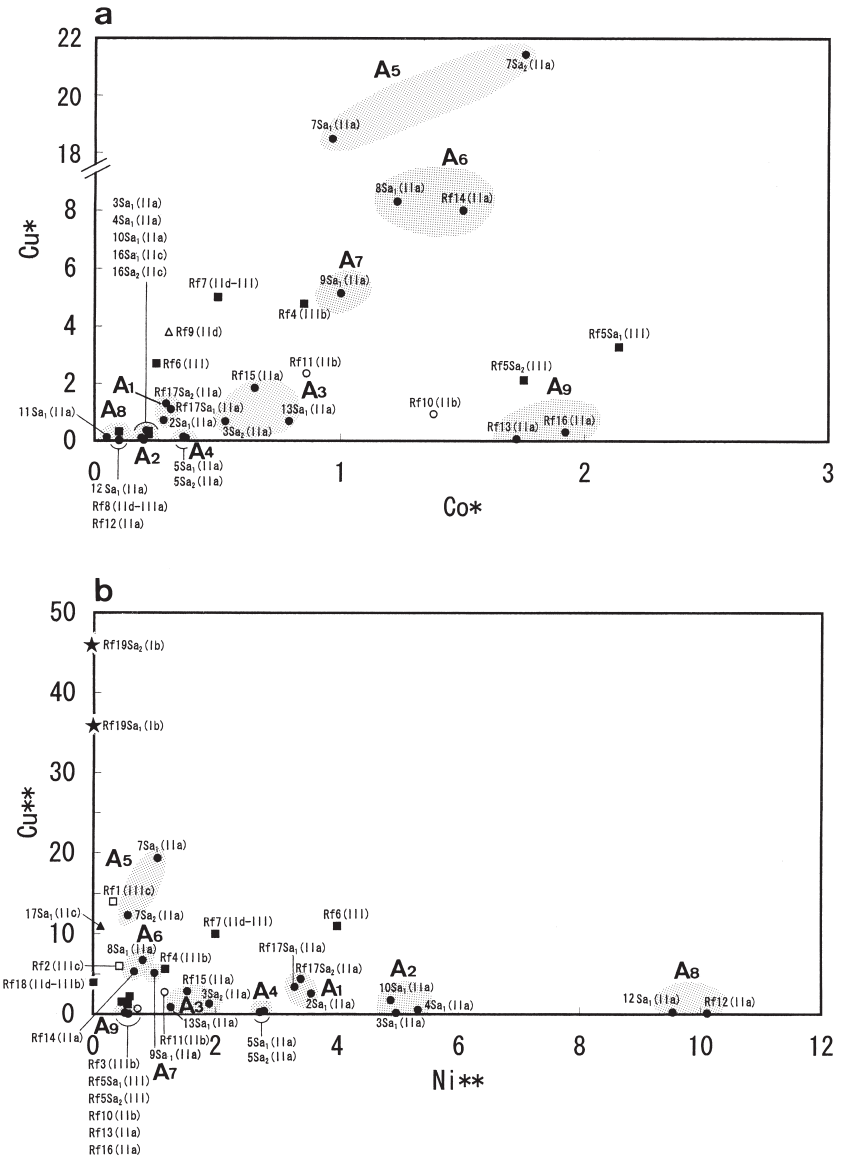

Fig.9 Relationship between Co* [the values of (mass%Co) / (mass%Ni)] and Cu* [the values of (mass%Cu) / (mass%Ni)] and between Ni** [the values of (mass%Ni) / (mass%Co)] and Cu** [the values of (mass%Cu) / (mass%Co)] in the iron artifacts and iron ore excavated from Stratum IIIc to Stratum IIa. The plots with numbers are analytical results in this paper. The others are results from previous studies: Rf1, Rf2, and Rf19 (Akanuma 2003), Rf3 to Rf10 and Rf13 to Rf16 (Akanuma 2005), Rf11 and Rf12 (Akanuma 2002), and Rf18 (Akanuma 2004). Stratum IIIc samples are expressed with open squares (□), Stratum IIIb, III, IId-III, IId-IIIb, and IId-IIIa samples by solid squares(■), Stratum IId samples by an open triangle (△), Stratum IIc samples by solid triangles (▲), Stratum IIb samples by open circles (○), Stratum IIa samples by solid circles (●),and Kültepe Ib samples by solid stars (★).

Sample No.1, described later as being iron ore, has 67.61mass% T.Fe and 2.84mass% FeO. The contents of Cu, Ni, and Co are less than 0.005mass% and the content of As is 0.01mass%. This result agrees with the EPMA analysis. Sample No.6, iron slag, has 50.03mass% T.Fe. This result shows that considerable amounts of iron oxide could have been generated in the smelting, refining, or forging process.

5-2 Metallographic examination of iron artifacts

Sample No.7, a pin-like object (Fig.2$a_{1\text{-}1}$), was covered with a layer of corrosion. Metallic iron remained in the inner portion, No.7Sa_1, so it was etched with nital. The macrostructure is etched almost

uniformly (Fig.2$a_{2\text{-}1}$). The microstructure (the area 'R_1' in the macrostructure) consists mainly of coarse-grained ferrite and a small amount of pearlite. It appears to have been air-cooled from a temperature above 723°C and its carbon content is estimated to be approximately 0.1mass% to 0.2mass%, based on comparison of the structure of standard carbon steel (Fig.2$a_{2\text{-}2}$). Sample No.13 Sa_1 (Fig.2$b_{1\text{-}1}$) has almost the same structure. The area marked 'R_1' in the macrostructure consists almost entirely of ferrite grains (αFe), or contained small amounts of carbon (Figs.2$b_{2\text{-}1}$ and 2$b_{2\text{-}2}$). The carbon content estimated from this structure is approximately 0.1mass% or below.

The macrostructure of Sample No.7Sa_2 is almost completely composed of corrosion (Fig.2$a_{3\text{-}1}$). There are many voids and cracks in this structure. In the EPMA backscattered electron image (BEI) of the area 'R_1' in that macrostructure, fine crystals (Cm) with a metallic luster, and their holes, are observed (Fig.2$a_{3\text{-}2}$). These crystals are believed to be cementite (Fe_3C) in pearlite[3] because the main components are Fe and C as seen by the elemental distribution mapping by EPMA (Fig.2$a_{3\text{-}3}$). The cementite is separated out along the ferrite grain boundaries in the metal before corroding. The carbon content of Sample No.7Sa_2 estimated from this structure is between 0.1mass% and 0.2mass%; this is based on the area ratio occupied by these crystals and their holes in the microstructure. Samples No.7 and No.13 are estimated to be mainly low carbon steel, which is better suited for producing iron artifacts with complicated forms. Structures with almost the same composition were found in Sample No.4Sa_1 (Figs.3b_1 to 3b_3), which also has an estimated carbon content of between 0.1mass% and 0.2mass%. In the microstructures of Samples No.2Sa_1, No.3Sa_1, No.10Sa_1, No.11Sa_1, and No.16Sa_1・Sa_2, areas consisting of crystals with a metallic luster or their holes forming lamellar structures are observed (Figs.3a_1 to 3a_3, Figs.4$a_{1\text{-}1}$ to 4$a_{2\text{-}2}$, Figs.5c_1 to 5c_3, Figs.5d_1 to 5d_4, and Figs.6$b_{1\text{-}1}$, 6$b_{2\text{-}1}$ to 6$b_{2\text{-}3}$, 6$b_{3\text{-}1}$, and 6$b_{3\text{-}2}$).The estimated carbon content of Samples No.2Sa_1 and No.11Sa_1 is between 0.3mass% and 0.4mass%, and that of No.16Sa_1・Sa_2 is between 0.2mass% and 0.3mass%. It is difficult to estimate the carbon contents of Samples No.3Sa_1 and No.10, as the distribution of cementite or its holes in the macrostructures is not clear.

Samples No.7Sa_1 and No.13Sa_1 have non-metallic inclusions with light gray and granular areas (IO) and dark areas (Gl) (Figs.2$a_{2\text{-}3}$ and 2$b_{2\text{-}3}$). The light gray area is believed to be wüstite, and the dark area (Gl) is a glassy silicate mainly consisting of FeO, CaO, Al_2O_3, and SiO_2 (Figs.2$a_{2\text{-}4}$ and 2$b_{2\text{-}4}$). A non-metallic inclusion with the same mineral composition is found in Sample No.16Sa_1 as shown in Figs.6$b_{2\text{-}4}$ and 6$b_{2\text{-}5}$. Non-metallic inclusions with dark areas are present in Samples No.3Sa_2, No.5Sa_1, No.9Sa_1, No.11Sa_1, and No.17Sa_1 (Figs.4$a_{3\text{-}1}$ to 4$a_{3\text{-}3}$,Figs.4$b_{1\text{-}1}$ to 4$b_{2\text{-}3}$, Figs.5b_1 to 5b_4, Figs.5d_2,5d_5,and 5d_6, and Figs.6$a_{1\text{-}1}$, 6$a_{2\text{-}1}$,6$a_{2\text{-}4}$, and 6$a_{2\text{-}5}$, Table 4). As seen in Table 4, the composition of each non-metallic inclusion is different. In particular, No.3Sa_2 and No.5Sa_1 have MnO contents exceeding 9mass%. Many minute non-metallic inclusions with almost the same chemical composition are present in No.5Sa_1, which also contains 0.083mass% Mn (Table 2). This high Mn content is generally believed to arise from these non-metallic inclusions. CaO contents between 8.91mass% and 17.0mass% are detected in the non-metallic inclusions of Samples No.5Sa_1, No.11Sa_1, and No.17Sa_1. The Ca-rich inclusions may originate from manufacturing processes.

Samples No.8Sa_1 and No.17Sa_1 have many voids and cracks. Minute grains with metallic luster are found in the iron corrosion of their macrostructures. EPMA analyses reveal that they are mainly composed of copper (Figs.5a_1 to 5a_4 and 6$a_{2\text{-}1}$ to 6$a_{2\text{-}3}$). These two samples each contain more than 0.1mass% Cu; these chemical compositions conform well the microstructures.

Due to the advanced states of corrosion of Samples No.5Sa_2, No.12Sa_1 (Fig.5e_1), No.14Sa_1 (Fig.6$c_{1\text{-}1}$), and No.15Sa_1 (Fig.6$d_{1\text{-}1}$), their carbon contents could not be estimated, and non-metallic inclusions were not found.

[3] Similar crystals with a metallic luster discovered in a dagger were identified as cementite in an archaeometallurgical analysis of the crystals (Knox 1963)

Table 3 Composition of iron ore and iron slag by ICP-OES, IRA, and EPMA

No.	Sub. No.	chemical components(mass%)																three elements ratios				mineral composition
		T.Fe	FeO	Cu	Ni	Co	Mn	P	Ti	Si	Ca	Al	Mg	V	As	Sb	Mo	Cu/Ni	Co/Ni	Cu/Co	Ni/Co	
1	Sa_1	67.61	2.84	0.004	<0.001	0.003	0.019	0.05	0.011	0.82	0.118	0.164	0.037	0.010	0.01	<0.01	0.003	-	-	-	-	Hem
6	Sa_1	50.03	-	0.006	<0.001	0.002	0.646	0.07	0.019	4.33	2.23	0.379	0.301	0.014	<0.01	<0.01	0.001	-	-	-	-	IO(W s), Gl
Rf18	-	51.81	-	0.772	0.003	0.196	0.003	<0.01	0.004	3.16	0.603	0.241	0.346	0.028	0.23	<0.01	<0.001	-	-	<0.01	3.94	Hem, Gt

The numbers refer to sample descriptions in Table1.FeO was analyzed assuminig that the content of M・Fe (metallic iron) was zero.
Hem:hematite, Gt:goethite, IO:Fe-O system compound (believed to be wüstite), Gl: a glassy silicate.

Table 4 Chemical Composition found in the non-metallic inclusions in the iron artifacts by EPMA

No.	L	chemical components (mass %)										total
		MgO	Al_2O_3	SiO_2	CaO	TiO_2	V_2O_5	MnO	FeO	P_2O_5	K_2O	Na_2O	
No.3Sa_2	Gl_1	1.08	11.6	41.0	1.69	0.38	-	12.5	27.6	-	2.84	0.60	99.29
	Gl_2	1.55	9.95	39.2	1.45	0.32	-	13.2	31.2	-	2.44	0.46	99.77
No.5Sa_1	Gl_1	4.28	10.8	52.7	13.7	0.69	-	9.32	3.09	-	4.65	0.25	99.48
	Gl_2	4.20	10.9	53.2	13.7	0.69	-	9.56	3.11	-	4.17	0.20	99.73
No.11Sa_1	Gl	1.32	12.1	50.9	8.91	0.64	0.22	< 0.01	22.5	0.06	2.87	0.66	100.18
No.17Sa_1	Gl	1.99	10.0	62.2	17.0	0.22	0.03	< 0.01	3.03	-	3.95	1.55	99.97

L corresponds to the locations in Figs.4 to 6.

5-3 Metallographic examination of ore and slag

Sample No.1 is a roughly hemispherical lump weighing 413g and having weak magnetism (Fig.7a_1). The marked area of the macrostructure consists of gray and dark gray areas (Figs.7b_1 and c_1). In the EPMA analysis of these two areas, the peak profiles of Fe-Lα and Fe-Lβ are almost the same as the profiles of a standard sample of hematite (Fig.7d_1). The chemical composition of this sample, especially T.Fe and FeO (Table 3), indicates the predominant constituents are hematite and a small amount of magnetite.

Sample No.6 is a lump of dark brown slag with red-brown iron corrosion (Fig.8a_1). There are many voids in the macrostructure (Fig.8b_1). The marked area in Fig.8b_1 consists of iron oxide (IO), dark-gray areas (Gl), and dark areas (Ma) (Fig.8c_1). The area (IO) is identified as wüstite based on the state analysis by EPMA (Fig.8d_1). The area (Gl) is a glassy area whose main components are FeO, CaO, Al_2O_3, and SiO_2. The dark area (Ma) is composed of a glassy silicate with minute crystals in it (Figs.8c_1 and 8c_2).

6 DISCUSSION

6-1 Composition of iron ore and iron slag from Stratum IIIb to IIa

It has been ascertained that Sample No.1 from Stratum IIIb is a lump of hematite containing a small amount of magnetite. Little gangue minerals are contained in this sample. It was not found in association with any signs of iron production activity. It may have been used as red pigment for decorating materials such as pottery,[4] rather than a raw material to be used for iron smelting. Another small lump of iron ore (Rf18) composed mainly of hematite and goethite was excavated from a Stratum IIIb/IId level (Akanuma 2004). This sample is also thought to have been used as pigment. As seen in Table 3, Sample Rf18 has higher Cu, Co, and As contents than Sample No.1. This indicates that iron ore may have been brought from multiple areas during the period represented by Stratum IIIb/IId.

[4] A large amount of pottery with red or dark reddish-brown decoration has been discovered at the site (Omura 2002).

Sample No.6 is iron slag whose main components are Fe, Si, and Ca. Many particles consisting of FeO and iron grains were observed in the macrostructure. It is almost certain that Sample No.6 represents a state in which molten or partially molten slag was in contact with metallic iron. A progressive increase in the deposits of iron artifacts, lumps, and slag is seen in the excavation layers of Stratum IIa. The discovery of Sample No.6 is further evidence of metallurgical activity at the site during this period.

6-2 Composition of iron artifacts from Stratum IIIc to IIa

According to the author's archaeometallurgical analysis of iron objects from Kaman-Kalehöyük, ironware made of steel has been discovered in each stratum from Stratum IIIc to Stratum IIa, spanning the 2nd and 1st millennia B.C. In many cases, the steel used for manufacturing that ironware had less than 0.5mass% carbon. There were also a few samples with a carbon content estimated to be more than 0.5mass% (Akanuma 2003; 2005). This indicates that steel with different carbon contents may have been produced deliberately during the 2nd and 1st millennia B.C. This matter should be clarified by further examination.

At least three manufacturing processes are needed to produce iron (steel): smelting, refining, and forging. It is difficult to say which of these operations were performed at Kaman-Kalehöyük during each cultural period spanning the 2nd and the 1st millennia B.C., since structures and tools related to iron production activities have not yet been discovered at the site. It is certain that steel to be used for manufacturing objects was produced in a multistage process. Even if the same raw materials are used to make iron as a starting material, different manufacturing methods and production conditions can produce a difference in the composition of the final steel product. Therefore, it is not useful to classify archaeological objects by direct comparison of chemical compositions. It is necessary to direct our attention instead to the trace elements that are believed to reflect the composition of the raw materials without being influenced by manufacturing methods and conditions, corrosion, or contamination from the soil.

As discussed in section 5-1, Ti, Mn, P, and As may be contaminants from the surrounding soil. Since a large amount of slag related to copper production activity has been found at this site (Masubuchi and Nakai 2005), it is believed that high As contents originate from soil pollution associated with this activity. This should be clarified by further research.

The elements Ni, Co, and Cu are believed to remain in the metallic iron throughout the processes of smelting, refining, and forging (Akanuma 2002; 2003). It is also suggested that Ni, Co and Cu content are minimally influenced by burial deposits. Therefore, we can believe that the concentrations of Ni, Co, and Cu in the samples reflect the original compositions of the objects themselves. Although there is variation in the absolute content of these trace elements from artifact to artifact, the concentration ratios in the archaeological objects should be similar to those in the raw materials used to produce the objects, provided no additional alloying was carried out.

The values of (mass%Co)/(mass%Ni) and (mass%Cu)/(mass%Ni) were calculated for the iron artifacts that contained more than 0.005mass% Ni. Also the values of (mass%Ni)/(mass%Co) and (mass%Cu)/(mass%Co) were calculated for the samples containing more than 0.005mass% Co. The calculated results are listed in Table 2. The relationship between the values of (mass%Co)/(mass%Ni) and (mass%Cu)/(mass%Ni), and the values of (mass%Ni)/(mass%Co) and (mass%Cu)/(mass%Co) are indicated on Figs.9a and 9b. In these figures, another eighteen iron artifacts and one lump of iron ore found in Stratum III and Stratum II levels are also plotted. The archaeometallurgical analysis of these nineteen iron objects (Rf1 to Rf19) was documented previously (Akanuma 2002; 2003; 2004; 2005). In Fig. 9b, the analysis of two samples from an artifact excavated from the Karum Ib level at Kültepe (Akanuma 2003) are also plotted. The date of the Kültepe object is almost equivalent to that of the three objects from Kaman-Kalehöyük Stratum III. The plots of this sample ($Rf19Sa_1$ and $Rf19Sa_2$) are symbolized by a solid star (★). Stratum IIIc samples are expressed with open squares (□), Stratum IIIb, III, IId-III, and IId-IIIa samples by solid squares (■), Stratum IId samples by an open triangle (△), Stratum IIc samples by solid triangles

(▲), Stratum IIb samples by open circles (○), and Stratum IIa samples by solid circles (●). Sample No.14 (belonging to IIc) could not be plotted because of its low Ni and Co contents (under 0.005mass%).

Samples excavated from Stratum IIa cluster in nine groups (A1 to A9) in Figs.9a and 9b. The distribution domains of six other samples fall outside of those nine groups: Samples Rf10 and Rf11 from Stratum IIb, Samples Rf5 and Rf6 from Stratum III, and Samples Rf3 and Rf4 from Stratum IIIb. These analytical results indicate that smelted iron, smelted and refined iron, or iron artifacts as final products were brought to the site of Kaman-Kalehöyük from multiple regions during the period spanning Stratum IIIb to Stratum IIa.

The samples excavated from Stratum IIIc (Samples Rf1 and Rf2) and the samples from Kültepe Ib ($Rf19Sa_1$ and $Rf19Sa_2$) have characteristic chemical compositions in that the Co content is higher than the Ni content (ten or twenty-five times higher Co than Ni in the Kültepe samples and two or three times higher Co than Ni in the Stratum IIIc samples) compared to the 28 samples from Kaman-Kalehöyük, except for $No.17Sa_1$. Since features related to iron production activity, such as furnaces, tools, or slag, have not been found in Stratum IIIc at Kaman-Kalehöyük, it is difficult to hypothesize that Samples Rf1 and Rf2 were produced at this site. Considering that archaeological objects with Mesopotamian characteristics have been found in Stratum IIIc,[5] we should investigate the exchange of iron-related material culture between Anatolia and Mesopotamia. Sample $No.17Sa_1$ plots near Sample Rf1 in Fig.9b; there may be similarities in the acquisition routes of these samples to the site of Kaman-Kalehöyük.

Sample $No.3Sa_1$ plots in the area of Group A2. On the other hand, Sample $No.3Sa_2$ from the same object is located in Group A3. This indicates that steel with different chemical compositions may have been used deliberately to manufacture Sample No.3. It is possible that two or more kinds of steel manufactured from different raw materials, or reused from different periods, were used to produce Sample No.3. This matter should be clarified by additional research.

7 CONCLUSION

It is thought that the change from bronze to iron in the Near East came about through the diffusion of iron production technology developed by the Hittite Empire to the surrounding regions after the downfall of the Hittite Empire (cf. Tsumoto 2004). However, the archaeological and archaeometallurgical studies of iron objects excavated from the site of Kaman-Kalehöyük suggest that steel production had already been established before the Hittite Empire Period.

From Figs.9a and 9b, we can hypothesize that iron was produced in more areas in the cultural age of Stratum IIa compared to previous periods. Iron products and iron slag have been excavated in larger amounts from Stratum IIa in comparison to earlier levels. These results indicate that about four hundred years after the downfall of the Hittite Empire, the use of iron products pervaded everyday life in the region of Kaman-Kalehöyük.

In order to clarify the details of the origin, development, and establishment of iron culture in Anatolia during the 2nd and 1st millennia B.C., we have to investigate the exchange of material culture with Mesopotamia in the 3rd and 2nd millennia B.C., reexamine the role of the Hittite Empire in iron production, and continue to accumulate and examine archaeometallurgical data from Kaman-Kalehöyük and other sites.

ACKNOWLEDGEMENTS

The author is very grateful to Dr. Sachihiro Omura and all the members of the Kaman-Kalehöyük excavation team for their support of this study and useful suggestions. The author also appreciates the helpful comments of Dr. Kimihisa Ito and Ms. Claire Peachey.

[5] Personal communication with Dr. Sachihiro Omura.

BIBLIOGRAPHY

Akanuma, H.

1995a"Metallurgical Analysis of Iron Artifacts and Slag Excavated from Kaman-Kalehöyük," *AAS* IV, pp.119-133 (in Japanese).

1995b"Metallurgical analysis of Iron Artifacts and Slag from Archaeological Site of Kaman-Kalehöyük," *BMECCJ* VIII, pp.59-88.

1999 "Production of Iron Materials during the Phrygian Period at Kaman-Kalehöyük: through a Scientific Analysis of the Iron Relics from the Results of the Twelfth Excavation," *AAS* VIII, pp.337-354 (in Japanese).

2001 "Iron Objects from Stratum II at Kaman-Kalehöyük: Correlation between Composition and Archaeological Levels," *AAS* IIX, pp.217-288.

2002 "Iron Objects from the Architectural Remains of Stratum III and Stratum II at Kaman-Kalehöyük: Composition and Archaeological Levels," *AAS* XI, pp.191-200.

2003 "Further Archaeological Study of 2nd and 1st millennium BC Iron Objects from Kaman-Kalehöyük," *AAS* XII, pp.137-149.

2004 "Archaeometallurgical Analysis of Iron and Copper Objects from Stratum III and Stratum II at Kaman-Kalehöyük: Correlation between Composition and Archaeological Levels," *AAS* XIII, pp.163-174.

2005 "The Significance of the Composition of Excavated Iron Fragments from Stratum III at the Site of Kaman-Kalehöyük, Turkey," *AAS* XIV, pp.147-157.

Knox, R.

1963 "Detection of Carbide Structure in the Oxide Remains of Ancient Steel," *Archaeometry* 6, pp.43-45.

Masubuchi, M. and I. Nakai

2005 "Scientific Analysis of Metallurgical Slag Excavated from Kaman-Kalehöyük (1)," *AAS* XIV, pp.183-194.

Omura, S.

1995 "A Preliminary Report on the Excavation at Kaman-Kalehöyük in Turkey (1989-1993)," *BMECCJ* VIII, pp.1-6.

1998 "A Preliminary Report on the Twelfth Excavation at Kaman-Kalehöyük (1997)," *AAS* VII, pp.1-84 (in Japanese).

2002 "Preliminary Report on the 16th Excavation at Kaman-Kalehöyük (2001)," *AAS* XI, pp.1-43.

2003 "Preliminary Report on the 17th Excavation at Kaman-Kalehöyük (2002)," *AAS* XII, pp.1-35.

2005 "Preliminary Report on the 19th Excavation at Kaman-Kalehöyük (2004)," *AAS* XIV, pp.1-54.

Tsumoto. H

2004 "Iron in Ancient West Asia: From Bronze to Iron," *Journal of West Asian Archaeology* 5, pp.11-23 (in Japanese).

Hideo Akanuma
Iwate Prefectural Museum
34 Uedamatsuyashiki, Morioka
Iwate 020-0102
Japan
akanuma@iwapmus.jp